A PARAMETRIC STUDY OF CURVED STRAKE ON SUPPRESSION OF HORSESHOE VORTEX DUE TO THE WING-BODY JUNCTION

***Chi-Wen Huang*[1]*, Jiahn-Horng Chen*[1]*, Ching-Yeh Hsin*[1]**
[1]*National Taiwan Ocean University, Department of Systems Engineering and Naval Architecture*
jhcntou@gmail.com

Abstract: *The horseshoe vortex due to a boundary-layer flow past a wing-body junction is common in engineering applications. The horseshoe vortex may result in vortical flow, non-uniform wake distribution, and noise signal and affect the efficiency of propulsor. Therefore, the development and suppression of the horseshoe vortex structure are vital engineering issues. In the present study, we introduced a strake to the wing-body junction and conducted a computational parametric study of the strake surface on the development of horseshoe vortex and investigate the effects of suppressing the vortex. The Spalart-Allmaras turbulence model was employed in the computation. The results were examined and we found that the horseshoe vortex can be significantly reduced and the wake flow much improved.*

Keywords: Horseshoe vortex, strake, wing-body junction.

Classification numbers: *2.1*

1. Introduction

Horseshoe vortex is an important three-dimensional phenomenon in junction flows which arise when a boundary layer passes an obstacle protruding from the body surface. It is quite common in engineering applications such as bridge piers on the river bed, the wing on the airplane body, and the sail on the submarine body. Various detrimental effects may be produced when the horseshoe vortex is present. Therefore, many studies on how to control it or mitigate its effects have been available in the literature.

Many control strategies have been proposed in the literature and can be roughly divided into two categories: active control and passive control. The latter seems more plausible in engineering applications. There are several approaches for this kind of control. The most common way is to improve the flow field by introducing some additional parts. For some examples, Batcho [1] suggested to employ a lifting structure which induces a positive lift so as to mitigate horseshoe vortices. Devenport and Dewitz [2] introduced a curved fillet and found by experiments that it could improve wake flow. Later, Zhang *et al.* [3-4] explained the mechanism of fillets by computational fluid mechanics (CFD). Liu *et al.* [5] employed a baffle to destroy the horseshoe vortex core so as to dissipate its energy and enhance the uniformity of wake flow. Liu and Xiong [6] later confirmed by CFD that the effect of baffle was better than that of fillet when applied to SUBOFF hull form. Recently, Younis *et al.* [7] adopted the vortex generator to develop counter vortices and the horseshoe vortex could be effectively suppressed in strength and size.

Devenport and Simpson [8] also proposed to implement a strake at the leading edge. They found that such a simple structure could reduce adverse pressure gradient and the boundary layer separation could be avoided. Nevertheless, Barberis *et al.* [9] argued that the effectiveness of strake on the control of horseshoe vortex was limited because it induced another horseshoe vortex. Fortunately, this view point has been clarified. Their arguments are only valid when the strake is not long enough [10].

The control of horseshoe vortex is a vital issue in many studies. Various methods have been proposed in the past several decades. Some of them could be effective but not easily realized in engineering applications. In fact, among these methods, fillets and strakes are the only two which have been implemented in submarines. This implies that these devices are applicable in engineering. In this study, we will focus on the horseshoe vortex control by a strake. Lee *et al.* [10] have shown that both linear and elliptical strakes can effectively suppress the vortex as long as their length is long enough. However, the linear strake could induce another vortex at the wing-strake junction. The present study will extend the previous research by varying the shape of the strake and explore the possible optimal shape for the particular wing studied here.

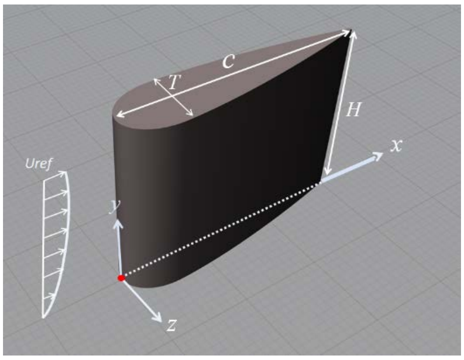

***Figure 1**. Schematic of flow field.*

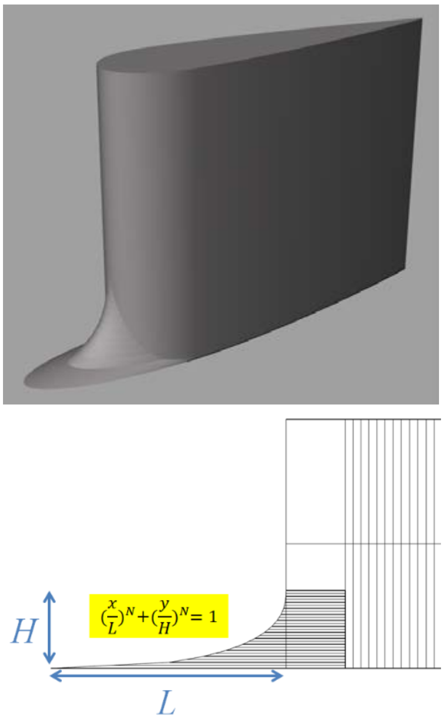

***Figure 2**. Schematic of the strake.*

2. Physical Model and Numerical Method

Shown in Figure 1, a flat-plate boundary layer passes a three-dimensional wing mounted on the flat plate. The angle of attack is 0°. The cord length is *C*, the wing span is *H*, and the maximum thickness is *T*. A Cartesian coordinate system is specified with its origin at the leading edge of junction.

The streamwise direction is *x*, span direction *y*, and lateral direction *z*.

The flow is incompressible and turbulent and must satisfies

$$\frac{\partial \bar{u}_i}{\partial x_i}=0 \tag{1}$$

$$\rho\bar{u}_j\frac{\partial \bar{u}_i}{\partial x_j}=-\frac{\partial \bar{p}}{\partial x_i}+\mu\frac{\partial^2 \bar{u}_i}{\partial x_j \partial x_j}-\frac{\partial}{\partial x_j}\left(\rho\overline{u_i' u_j'}\right) \tag{2}$$

Where ρ denotes the fluid density, u_i the velocity with $(u_1 \quad u_2 \quad u_3)=(u \quad v \quad w)$, p the fluid static pressure, and μ the fluid viscosity. The terms with an overbar represents time-averaged quantities. The coordinate system is $(x_1 \quad x_2 \quad x_3)=(x \quad y \quad z)$. The last term in Eq. (2) is the Reynolds stress tensor in which u_i' is the fluctuating velocity component. The Reynolds stress must be modelled by turbulence models. There have been many choices available in the literature. In the present study, we employed the Spalart-Allmaras model [11]. This is a low-order simple model. Nevertheless, our previous study show that it is highly accurate and computationally robust for the flow which we will study below [12].

In our study, the wing is composed by a 3:2 ellipse and the NACA 0020 section. The joins together at the maximum thickness. The wing shown in Figure 1 is implemented with a strake with geometry shown in Figure 2. The height of the strake is *H* and length *L*. The level curve describing the strake is

$$\left(\frac{x}{L}\right)^N+\left(\frac{y}{H}\right)^N=1 \tag{3}$$

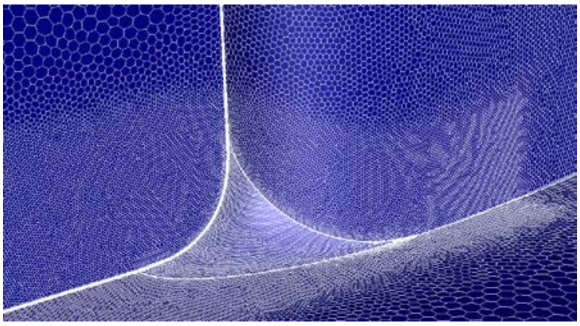

***Figure 3.** Mesh near the strake.*

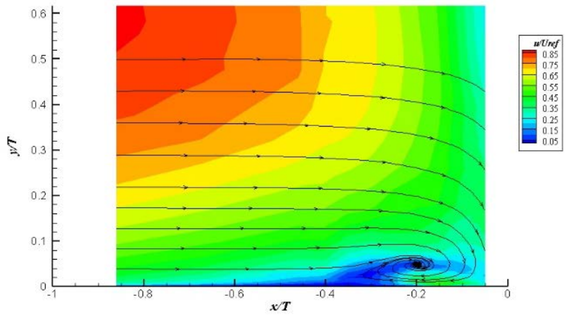

(a) Horseshoe vortex in experiment [18].

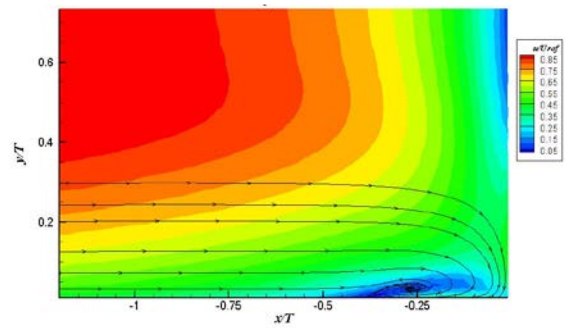

(b) Horseshoe vortex in our computation.

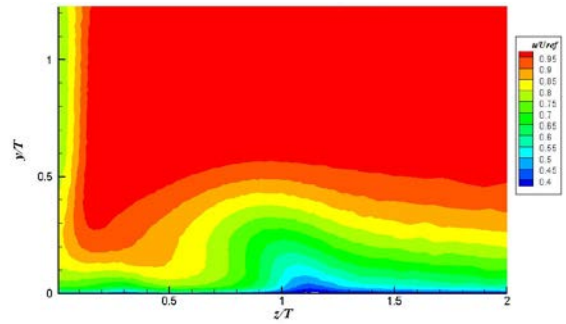

(c) Wake at x/C = 1.5.

Figure 4. *Flow field without a strake.*

This is a generalized ellipse. We can change the steepness of a strake by changing the value of *N*. In the present study, we chose *N* to be 1.5, 2.0, 2.5, and 3.0. Our previous investigation showed that the strake could effectively suppress the horseshoe vortex if $L/H \geq 2$. Therefore, we set $L/H = 3$ and 1 here.

The study was conducted computationally. The commercial software ANSYS was employed. The governing equations were discretized by the finite volume mehtod. The pressure and velocity fields were iteratively computed by the SIMPLE algorithm. Figure 3 shows the local unstructured hexahedral mesh used in our study. The total grid number is between 200M and 300M.

3. Results and Discussion

First of all, we compared our results with the experimental results available in the literature. igure 4(a) shows the experimental results by Devenport and Simpson [13]. The horseshow vortex can be clearly observed. The center is at $(x/T,\ y/T) = (-0.2,\ 0.05)$. Figure 4(b) shows our computations. The vortex is quite similar to the experimental resutls. The vortex core is somewhat more upstream at $(x/T,\ y/T) = (-0.28,\ 0.04)$. Furthermore, Figure 4(c) shows the wake flow at $x/C = 1.5$ in our computation. The low speed region at $z/T = 1.0$ is due to the horseshoe vortex developed upstream.

3.1. *L*/*H* = 1.0

Figures 5-8 show the computational results for different values of *N* and *H*/*T*. For each particular value of *N*, the vortex is stronger if the value of *H*/*T* is smaller. This can be observed if we compare parts (a) and (d) for each figure. This indicates that a small strake cannot effectively suppress the horseshoe vortex.

For a particular value of *H*/*T*, the low-speed region upstream of the wing becomes bigger if the *N* is bigger. This implies that for *L*/*H* = 1, *N* should not be large if we want to suppress the vortex or *H*/*T* should not be small.

Therefore, the curvature of strake plays a key factor for the appearance of the horseshoe vortex. If it is small enough, then the vortex can be suppressed. On the other hand, if it is too big, then the horseshoe vortex appears.

Figure 9 exhibits the detailed streamlines in the enlarged area where the horseshoe vortex may appear. When *H*/*T* = 2.5, the vortex always exists for all values of *N*. Obviously, the vortex cannot be eliminated if the strake is too short. As *H*/*T* increases, the vortex is evidently decreased. At *H*/*T* = 0.5, a small vortex appears if *N* is bigger. However, if *H*/*T* keeps growing, the vortex vanishes.

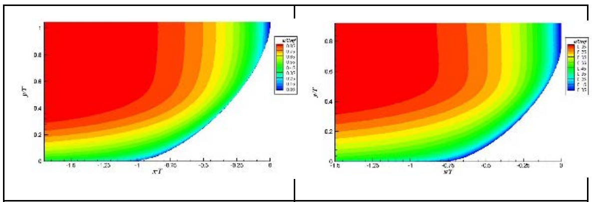

(a) H/T = 1.0	*(b) H/T = 0.75*

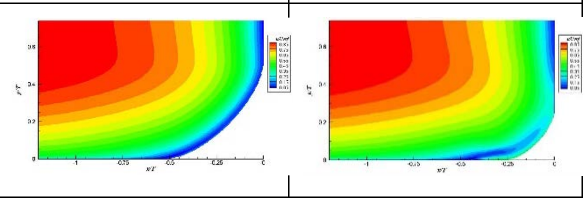

(c) H/T = 0.5	*(d) H/T = 0.25*

Figure 5. *Vortex development at N = 1.5.*

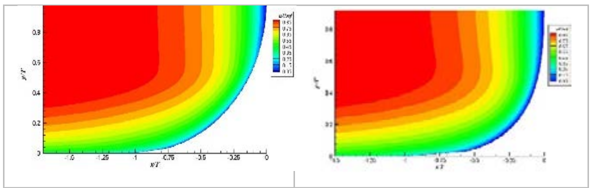

(a) H/T = 1.0	*(b) H/T = 0.75*

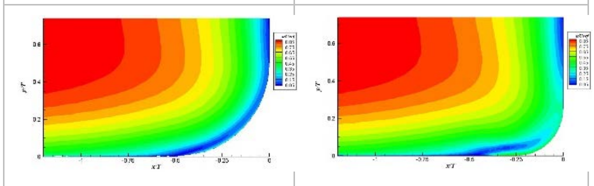

(c) H/T = 0.5	*(d) H/T = 0.25*

Figure 6. *Vortex development at N = 2.0.*

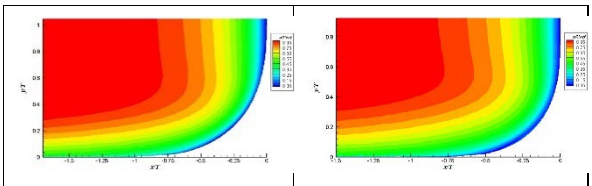

(a) H/T = 1.0	*(b) H/T = 0.75*

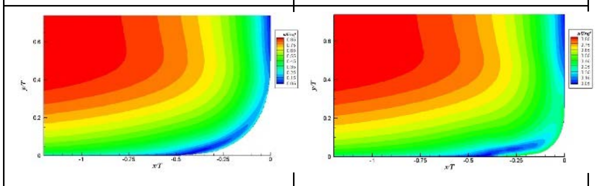

(c) *H/T* = 0.5	(d) *H/T* = 0.25

Figure 7. *Vortex development at N = 2.5.*

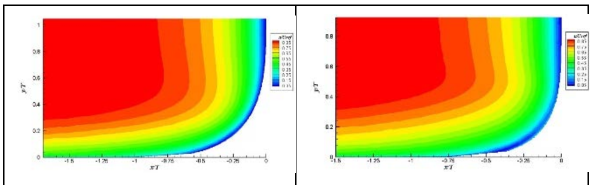

(a) H/T = 1.0	*(b) H/T = 0.75*

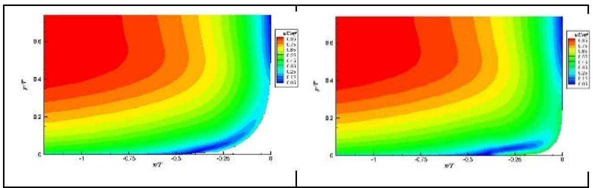

(c) H/T = 0.5	*(d) H/T = 0.25*

Figure 8. *Vortex development at N = 3.0.*

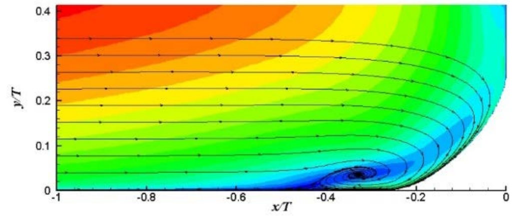

(a) N = 1.5, L/T = 1

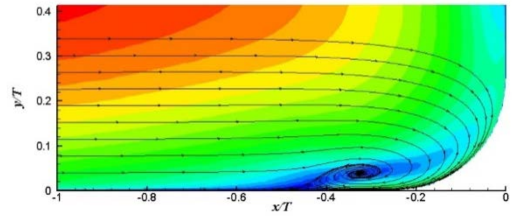

(b) N = 2.0, L/T = 1

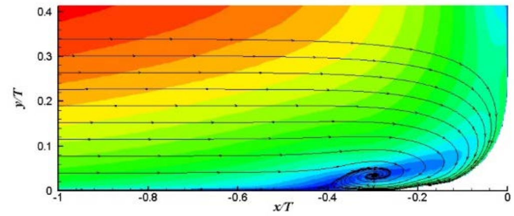

(c) N = 2.5, L/T = 1

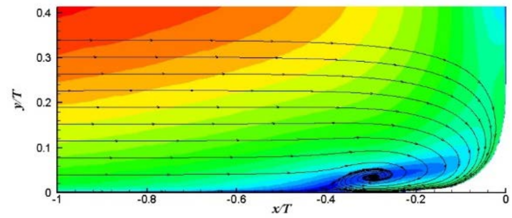

(d) N = 3.0, L/T = 1

Figure 9. *Detailed flow at H/T = 0.25.*

3.2. *L/H* = 3.0

Figures 10-13 show the computational results for different values of *N* and *H*/*T*. The curvature becomes smaller when *L*/*H* is bigger.

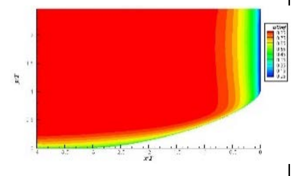

(a) H/T = 1.0

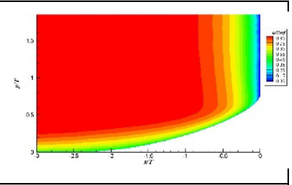

(b) H/T = 0.75

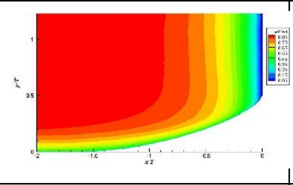

(c) H/T = 0.5

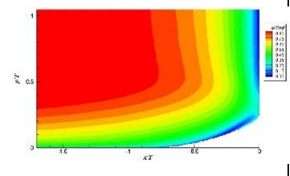

(d) H/T = 0.25

Figure 10. *Vortex development at N = 1.5.*

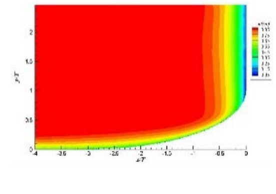

(a) H/T = 1.0

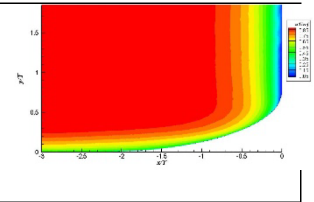

(b) H/T = 0.75

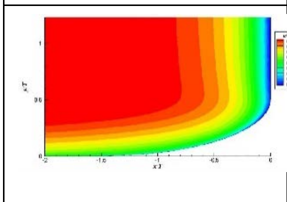

(c) H/T = 0.5

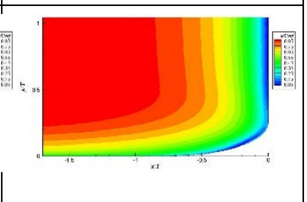

(d) H/T = 0.25

Figure 11. *Vortex development at N = 2.0.*

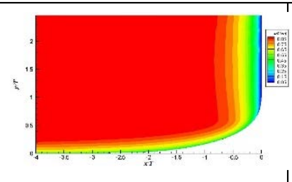

(a) H/T = 1.0

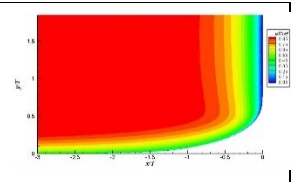

(b) H/T = 0.75

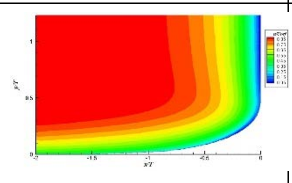

(c) H/T = 0.5

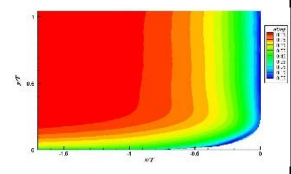

(d) H/T = 0.25

Figure 12. *Vortex development at N = 2.5.*

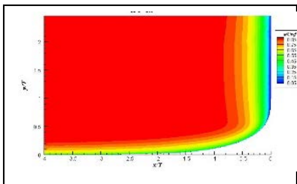

(a) H/T = 1.0

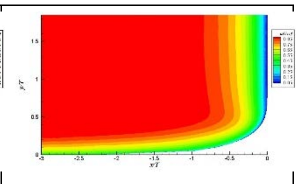

(b) H/T = 0.75

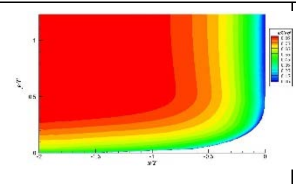

(c) H/T = 0.5

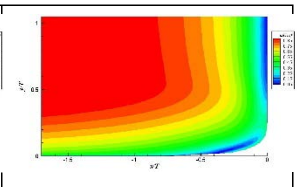

(d) H/T = 0.25

Figure 13. *Vortex development at N = 3.0.*

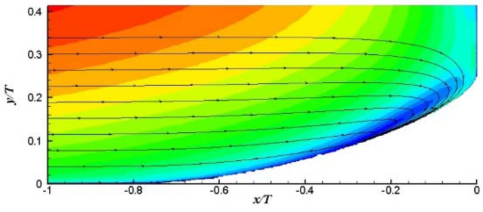

(a) N = 1.5, L/T = 3

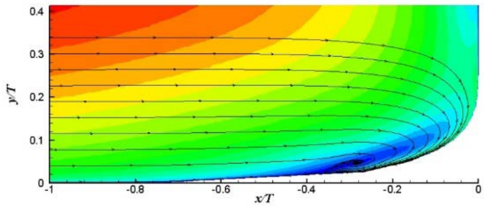

(b) N = 3.0, L/T = 3

Figure 14. *Detailed flow at H/T = 0.25.*

This benefits the flow around the strake. We can find that in all computations, the vortex is successfully eliminated. Even at $H/T = 0.25$, the minute vortex exists only when $N = 3$, as shown in Figure 13. A longer strake can help suppress the vortex. Therefore, the length of strake is an important parameter in vortex suppression.

Of course, if the value of H/T is small, the curvature of the strake is big and the low-speed region will be bigger. Consequently, if N is increased beyond some critical value, the vortex forms. Figure 13(b) is such a typical example; namely, N takes a big value, and H/T is not big enough. However, if we compare the results with those for $L/H = 1$.

According to the above observations, we find that the curvature is also an important factor for vortex control. One of the way to reduce curvature is to extend the length of the strake and at the same time, the strake height should be big enough. As to the value of N, its value should be too big. For the present wing, if N takes the value of 3, it would be too big.

2.3. Wake Improvement

The adoption of the strake help reduce the vortex in strength and size. A proper choice can even help suppress it. Since the horseshoe vortex is the main cause which makes the wake nonuniform, it is expectable that the wake would become more uniform when the horseshoe vortex is fully or partially suppressed.

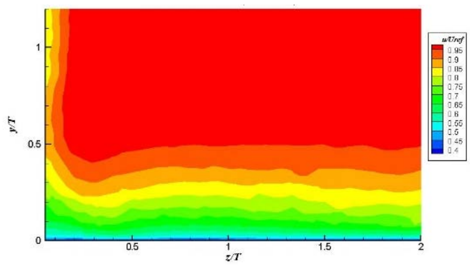

(a) H/T = 1

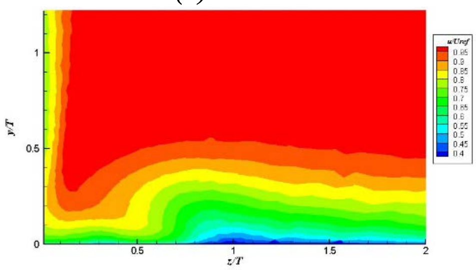

(b) *H*/*T* = 0.25

Figure 15. *Wake distribution at x/C = 1.5, L/H = 3 and N = 3.*

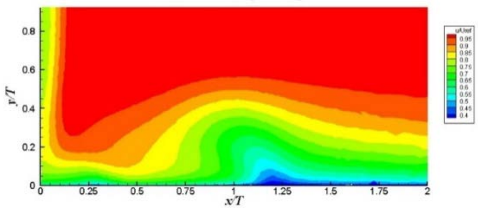

(a) H/T = 0.25, N = 2.0

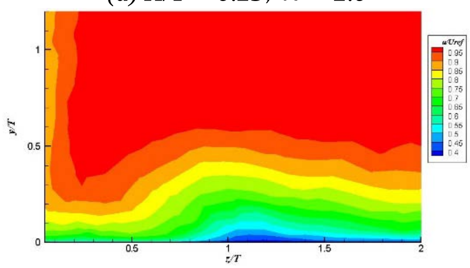

(b) H/T = 0.25, N = 3.0

Figure 16. *Wake distribution at x/C = 1.5, L/H = 1.*

Figure 15 shows the wake distributions at x/C = 1.5 for the wing implemented with a strake with N = 1.5 and L/T = 3. We may compare the results with that shown in Figure 3(c) which is due to the same wing without a strake and find that the wake is significantly improved. The conditions corresponding Figure 15(a) for which H/T = 1.0 lead to total suppression of horseshoe vortex and, therefore, we can find that the wake distribution is more uniform. There is almost no low-speed region. As to the result shown Figure 15(b) for which H/T = 0.25 and the horseshoe vortex is not totally suppressed, the wake flow is not so uniform even though the vortex is weakened in strength and size. It appears evident that the horseshoe vortex has strong effects on the wake development and distribution. One of the strategies to improve wake uniformity is to eliminate effectively the horseshoe vortex.

Figure 16 shows the results for short strake series (L/T = 1.0). In these cases, we learned in Sec. 3.1 that the horseshoe vortex is clearly present. Hence, it is expectable that the wake cannot be uniform. In fact, the computational results show that non-uniformity extends to even higher region. And the center of low-speed region moves between x/T = 1.0 and 1.25.

4. Conclusions

In the present study, we employ the CFD approach to study the effect of strake geometry on the development of horseshoe vortex. The level curves of the strake are generalized ellipses.

The study reveals that the length and curvature of strake are two important parameters to suppress the formation of horseshoe vortex. If the strake is enough long or its curvature is enough small, the implementation can effectively suppress the vortex. A stake is a simple device to be implemented in existing wing-body vehicles or structures. Our investigation also shows that the best value of N is 1.5 and 2.0.

In addition, we also find that the horseshoe vortex has significant effect on the wake non-uniformity. If the it can be totally suppressed, the wake can be significantly improved, which benefits the downstream flow development❑

References

[1] P.F. Batcho. *Method and apparatus for mitigating junction flows*, US Patent, US 6,186,445 B1 (2001).

[2] W.J. Devenport, N.K. Agarwal, M.B. Dewitz, R.L. Simpson, and K. Poddar. Effects of a fillet on the flow past a wing-body junction. *AIAA Journal*, Vol. **28**, (12), (1990), pp. 2017-2024.
[3] N. Zhang, H. Shen, and H. Yao. Validation of numerical simulation on resistance and flow field of submarine and numerical optimization of submarine hull form. *Journal of Ship Mechanics*, **9**, (1), (2005), pp. 1-13.
[4] N. Zhang, H. Shen, and H. Yao. Prediction of flow around submarine at different Reynolds numbers with Reynolds stress model. *Journal of Ship Mechanics*, **13**, (5), (2009), pp. 688-696.
[5] Z.-H. Liu, Y. Xiong, and C.-X. Tu. The method to control the submarine horseshoe vortex by breaking the vortex core. *Journal of Hydrodynamics, Series B*, **26**, (4), (2014), pp. 637-645.
[6] Z.-H. Liu and Y. Xiong. Comparison on the submarine horseshoe vortex control effects by vortex control bafflers and fillets. *Journal of Ship Mechanics*, **15**, (10), (2011), pp. 1102-1109.
[7] Y. Younis, H. Zhang, R. Zhu, and Z. Muhammad. Horseshoe vortex control using streamwise vortices, *Porcedia Engineering*, **126**, (2015), pp. 139-144.
[8] W.J. Devenport and R.L. Simpson. Flow past a wing-body junction: experimental evaluation of turbulence models. *AIAA Journal*, **30**, (4), (1992), pp. 873-881.
[9] D. Barberis, P. Molton, and T. Malaterre. Control of 3D turbulent boundary layer separation caused by a wing-body junction. *Experimental Thermal and Fluid Science*, **16**, (1-2), (1998), pp. 54-63 (1998).
[10] J.P. Lee, J.-H. Chen, and C.-Y. Hsin. Horseshoe vortex suppression due to a strake. 10th *International Workshop on Ship and Marine Hydrodynamics*, Keelung, Taiwan (2017).
[11] P.R. Spalart and S.R. Allmaras. A one-equation turbulence model for aerodynamic flows. *30th Aerospace Sciences Meeting and Exhibit*, Reno, Nevada (1992).
[12] J.P. Lee, J.-H. Chen, and C.-Y. Hsin. Study of junction flow structures with different turbulence models. *Journal of Marine Science and Technology*, **25**, (2), (2017), pp. 178-185.
[13] W.J. Devenport and R.L. Simpson. An experimental investigation of the flow past an idealized wing-body junction: final report. Report VPI-AOE-172, Virginia Polytechnic Institute and State University, Blacksburg, VA, USA (1990).

Ngày nhận bài: 28/2/2018
Ngày chuyển phản biện: 5/3/2018
Ngày hoàn thành sửa bài: 27/3/2018
Ngày chấp nhận đăng: 29/3/2018